Mice expressing minimally humanized CD81 and occludin genes support hepatitis C virus uptake *in vivo*

Running title: HCV uptake in entry factor knock-in mice

Qiang Ding[1], Markus von Schaewen[1], Gabriela Hrebikova[1], Brigitte Heller[1], Lisa Sandmann[2], Mario Plaas[3], Alexander Ploss[1, 4]

[1] Princeton University, Department of Molecular Biology, Lewis Thomas Laboratory, Washington Road, Princeton NJ 08544, USA

[2] Hannover Medical School, Hannover, Germany

[3] University of Tartu, Faculty of Medicine, Institute of Biomedicine and Translational Medicine, Laboratory Animal Centre, Ravila 14b, Tartu, Estonia, 50411

[4] To whom correspondence should be addressed: AP, aploss@princeton.edu

Abstract:

Hepatitis C virus (HCV) causes chronic infections in at least 150 million individuals world-wide. HCV has a narrow host range and robustly infects only humans and chimpanzees. The underlying mechanisms for this narrow host range are incompletely understood. At the level of entry differences in the amino acid sequences between the human and mouse orthologues of two essential host factors, the tetraspannin CD81 and the tight junction protein occludin (OCLN) explain at least in part HCV's limited ability to enter mouse hepatocytes. We have previously shown that adenoviral or transgenic overexpression of human CD81 and OCLN facilitates HCV uptake into mouse hepatocytes *in vitro* and *in vivo*. In efforts to refine these models we constructed knock-in mice in which the second extracellular loops of CD81 and OCLN were replaced with the respective human sequences, which contain the determinants that are critical of HCV uptake. We demonstrate that the humanized CD81 and OCLN are expressed at physiologic levels in a tissue-appropriate fashion. Mice bearing the humanized alleles form normal tight junctions and do not exhibit any immunologic abnormalities, indicating that interactions with their physiologic ligands are intact. HCV entry factor knock-in mice enable HCV uptake with similar efficiency as mice expressing HCV entry factors transgenically or adenovirally, demonstrating the utility of this model for studying HCV infection *in vivo*.

Importance:

At least 150 million individuals are chronically infected with hepatitis C virus (HCV). Chronic hepatitis C can result in progressive liver disease and liver cancer. New antiviral treatments can cure HCV in the majority of patients but a vaccine remains elusive. To gain a better understanding of the processes culminating in liver failure and cancer and to prioritize more efficiently vaccine candidates, small animal models are needed. Here, we describe the characterization of a new mouse model in which the parts of two host factors that are essential for HCV uptake, CD81 and occludin (OCLN) which differ between mice and men were humanized. We demonstrate that such minimally humanized mice develop normally, express the modified genes at physiological levels and support HCV uptake. This model is of considerable utility for studying viral entry in the three dimensional context of the liver and to test approaches aimed at preventing HCV entry.

Introduction:

Hepatitis C virus (HCV) is a positive sense, single stranded RNA virus belonging to the *Flaviviridae* family, genus hepacivirus (1). HCV progresses to persistent infection in 70-80% of those individuals who become acutely infected (2). Chronic carriers are at risk of developing fibrosis, cirrhosis and hepatocellular carcinoma (HCC) if untreated. Over the few years very potent directly acting antivirals (DAAs) have been approved which can cure HCV infection in the majority of patients (reviewed in (3)). Despite these tremendous successes HCV disease burden has only marginally decreased in part due to the limited availability of curative drug regimens and the lack of a protective vaccine. It remains also incompletely understood why individuals who have been successfully treated and have progressed to advanced fibrosis remain at an elevated risk for developing HCCs. Both vaccine development and improving our understanding of HCV pathogenesis would greatly benefit from a small animal for hepatitis C (4).

HCV's host range is limited to productive infection in humans and chimpanzees. It remains mechanistically incompletely understood why HCV has such a narrow host range. In mouse cells the HCV life-cycle is blocked or inefficiently supported at multiple steps, in particular viral entry and HCV RNA replication (reviewed in (5)). A surprisingly large number of host factors have been shown to be important in the the uptake of HCV into human hepatocytes, including glycosaminoglycans (GAGs) present on heparan sulfate proteoglycans (HSPGs)(6), low-density-lipoprotein receptor (LDLR) (7), CD81 (8), scavenger receptor class B member 1 (SCARB1) (9), the tight junction (TJ) proteins claudin-1 (CLDN1) (10) and occludin (OCLN) (11, 12), the receptor tyrosine kinases epidermal growth factor receptor (EGFR) and ephrin receptor A2 (EphA2) (13), the cholesterol transporter Niemann-Pick C1-like 1 (NPC1L1) (14), transferring receptor 1 (TfR1) (15), the cell death-inducing DFFA-like effector b (CIDEB) (16) and E-cadherin (17). Of those, differences in the sequences of CD81 and OCLN between the murine and human orthologues can at least in part explain the lower efficiency of HCV uptake in rodent versus human cells. Specifically, residues

contained in the second extracellular loops of CD81 and OCLN, which have previously been shown to be critical for HCV entry are not conserved (18, 19). We have previously demonstrated that ectopic overexpressing of human CD81 and OCLN enables uptake into mouse cell lines of both hepatic and non-hepatic origin (12, 20). Both CLDN1 and SCARB1 are also required but orthologues from other non-human species, such as mouse or hamster, have been shown to support HCV entry. When CD81 and OCLN are overexpressed through adenoviral delivery (21) or transgenically (22) HCV can enter mouse hepatocytes *in vivo*. While such genetically humanized mice have proven to be useful to study HCV entry and to test approaches focussing on blocking HCV entry (21, 23-25) a shortcoming is the unphysiologically high expression level achieved by these heterologous expression approaches. Also, neither CD81 nor OCLN are uniquely expressed in the liver, but rather on all nucleated cells and all tight junctions, respectively. Thus, it would be desirable to refine these models and monitor HCV uptake under conditions when both entry factors are expressed at physiological levels. To address this point we constructed a novel genetically humanized mouse model in which the second extracellular loops of CD81 and OCLN were humanized. Mice harboring the humanized alleles develop normally and do not exhibit any overt phenotype. Transcripts of these chimeric alleles are expressed at physiological levels similar in pattern that resembles expression of the wild-type alleles. The humanized CD81 molecule appears to facilitate the endogenous functions of murine CD81 as the chimeric mice do not show any defects in B cell development observed in CD81 deficient mice. In mice containing the humanized OCLN allele tight junctions are formed normally indicating that the mutant version can carry out the physiologic functions OCLN as part of TJ complexes. We further demonstrate that mice expressing both the humanized CD81 and OCLN alleles support uptake of HCV in a dose dependent manner. HCV uptake is similar as compared to mice administered with adenoviruses expressing CD81 and OCLN and HCV entry factor transgenic mice. This new HCV entry factor knock-in model will be useful for future mechanistic studies focusing on HCV entry.

Materials and methods:

Generation of mice expressing humanized CD81 and OCLN alleles

Gene targeting constructs coding mCD81/hEL2 (mouse exons 6 and 7 of CD81 gene, coding extracellular loop named EL2, were replaced with human exons 6 and 7) and mOCLN/hEL2 (a part of exon 3 of mouse OCLN gene, that encodes extracellular loop 2, was replaced with a part of human exon 3, what code EL2) where transformed into ES cells (genetic background 129S6SvEv) by standard electroporation (**Fig. 1C and 1D**). Correct targeting of the alleles in ES cell clones was analyzed by PCR and verified by DNA sequencing. After checking the number of chromosomes, in vitro Cre-recombination was performed to cut of Neo-tk selection cassette between LoxP sites. Correctly targeted ES cell clones containing the mCD81/hEL2 or mOCLN/hEL2 alleles were microinjected into C57BL6/J blastocysts. Chimeric mice were initially crossed with C57BL6/J (in case of mOCLN/hEL2) mice or with 129S6SvEv mice (In case of mCD81/hEL2) to obtain germline offspring. mOCLN/hEL2 and mCD81/hEL2 knock-in mice were subsequently crossed for 10 generations to the C57BL/6 background. Experiments were performed in accordance to a protocol reviewed and approved by the Institutional Animal Care and Use Committee of the University of Tartu.

Animals and cell lines

Generation of mice expressing human HCV entry factors under the control of a liver specific albumin promoter was previously described (22). Gt(ROSA)26Sor$^{tm1(Luc)Kaelin}$ (26) (Rosa26-Fluc) were obtained from The Jackson Laboratory and backcrossed for 10 generations to the C57BL/6 background. Rosa26-Fluc mice contain the firefly luciferase (luc) gene inserted into the Gt(ROSA)26Sor locus. Expression of the luciferase gene is blocked by a loxP-flanked STOP fragment placed between the luc sequence and the Gt(ROSA)26Sor promoter. Cre recombinase mediated excision of the transcriptional stop cassette results in luciferase expression in Cre-expressing

tissues. Mice were bred and maintained at the Laboratory Animal Resource Center of Princeton University according to guidelines established by the Institutional Animal Committee. Huh-7.5 (kindly provided by Charles Rice, The Rockefeller University), Huh-7.5.1 (kindly provided by Frank Chisari, The Scripps Research Institute) were maintained in 5% and 293T (American Type Culture Collection, ATCC), and HEK293 (ATCC) in 10% fetal bovine serum (FBS) containing DMEM supplemented with 1% nonessential amino acids (NEAA).

Quantification of the humanized CD81 and OCLN transcripts by RT-PCR

Total RNA was isolated from mouse brain, heart, large and small intestine, kidney, liver, lung, skin, spleen and stomach using RNeasy Mini Kit (Qiagen, Valencia, CA). cDNA was synthesized form 0.5 µg RNA using a SuperScript III First-Strand Synthesis System (Invitrogen, Carlsbad, CA) according to manufacturers instructions. Quantitative PCR was performed with a STEP ONE PLUS RT-PCR System (Applied Biosciences) using an Applied Biosystems SYBR Green PCR Master Mix (Warrington, UK) and primer pairs listed in **table 1**.

HCV generation and infections

Huh-7.5.1 or Huh-7.5 cells were electroporated with *in vitro* transcribed full-length HCV RNA of the BiCre-Jc1 genomes (21). 72 hours post-electroporation, the medium was replaced with DMEM containing 1.5% FBS and supernatants were harvested every six hours starting from 72h. Pooled supernatants were clarified by centrifugation at 1,500 x g, filtered through a 0.45 □m bottle top filter (Millipore) and concentrated using a stirred cell (Millipore). Viral titers ($TCID_{50}$) were determined using Huh-7.5 cells as previously described (27).

Production of recombinant adenoviruses

Adenovirus stocks encoding human and murine homologues of the four HCV entry factors (CD81, SCARB1, CLDN1 and OCLN) were generated as previously described (28). Briefly, adenovirus constructs were transfected into HEK293 cells

(ATCC) using the calcium-phosphate method. Transfected cultures were maintained until cells exhibited complete cytopathic effect (CPE), then harvested and freeze-thawed. Supernatants were serially passaged two more times with harvest at complete CPE and freeze-thaw. For virus purification, cell pellets were resuspended in 0.01M sodium phosphate buffer pH 7.2 and lysed in 5% sodium-deoxycholate, followed by DNAse I digestion. Lysates were centrifuged and the supernatant layered onto a 1.2-1.46 g/ml CsCl gradient, then spun at 23,000 rpm on a Beckman Optima 100K-Ultra centrifuge using an SW28 spinning-bucket rotor (Beckman-Coulter). Adenovirus bands were isolated and further purified on a second CsCl gradient using an SW41.Ti spinning-bucket rotor. Resulting purified adenoviral bands were isolated using a 18.5G needle and twice-dialyzed against 4% sucrose. Adenovirus concentrations were measured at 10^{12} times the dilution factor times the OD260 reading on a FLUOstar Omega plate reader (BMG Labtech). Adenovirus stocks were aliquoted and stored at -80ºC.

Antibodies and Flow Cytometry Analysis.

Bone marrow, spleen and thymus were harvested from mice of the indicated genotypes and homogenized through a cell strainer. For isolation of splenocytes, the spleen was digested in collagenase-containing medium for 30 minutes at 37°C previous to homogenization. Peritoneal cavity cells were obtained by peritoneal lavage with ice-cold PBS. Cell suspensions were first incubated with anti-CD16/CD32 mAb (BD Pharmingen, 553141, clone 2.4G2) for 15 minutes at 4°C. Following the blocking step cells were incubated with flourochrome- or biotin-conjugated antibodies for 30 minutes at room temperature. Splenocytes, bone marrow and peritoneal cavity cells were stained with FITC anti-mouse CD5 (BioLegend, 100605, clone 53-7.3, 1:100), PerCP-Cy5.5 anti-mouse CD19 (eBioscience, 45-0193-82, clone 1D3, 1:100), APC anti-human CD81 (BD Pharmigen, 551112, clone JS-81, 1:100), Alexa700 anti-mouse CD45R/B220 (Invitrogen, RM2629, clone RA3-6B2, 1:100), APC-Cy7 anti-mouse IgM (BioLegend, 406515, clone RMMM-1, 1:100), biotin anti-mouse CD81 (Novus Biologicals, NBP1-28138, clone 2F7, 1:100) and PE-Cy7 anti-mouse CD11b

(eBioscience, 15-0112-82, clone M1/70, 1:199). Splenocytes and thymocytes were stained with FITC anti-mouse CD81 (Miltenyi Biotec, 130-094-864, clone EAT2, 1:50), PE-TxRed anti-mouse CD4 (Abcam, ab51467, clone GK1.5, 1:50), APC anti-human CD81 (BD Pharmingen, 551112, clone JS-81, 1:100), Alexa700 anti-mouse CD45R/B220 (Invitrogen, RM2629, clone RA3-6B2, 1:100), APC-Cy7 anti-mouse CD3 (BD Pharmingen, 557596, clone 145-2C11, 1:100) and PE anti-mouse CD8 (BD Pharmingen, 553089, clone 53-6.7, 1:100). Biotin-conjugated reagents were counterstained with streptavidin-R-PE (Qiagen, 922721, 1:500). Samples were washed and resuspended in 100 µl PBS. Finally flow cytometry was performed with BD LSRII Flow Cytometer (BD Bioscience) and FlowJo Software (Tree Star, San Carlos, CA, USA) was used for data analysis.

Histology

Mice was euthanized, the liver perfused with PBS, extracted. The tissues were subsequently fixed overnight in 4% paraformaldehyde at 4°C with gentle agitation then dehydrated overnight in cryoprotection solution (30% sucrose solution PBS) at 4°C with gentle agitation before embedded in OCT for frozen sectioning. Cyrosections of 6 µm thickness liver were cut on a microtome and treated with solution containing 5% BSA and 0.5% Triton-X100 for 1h for blocking and permeabilization. Liver sections were stained with anti-Claudin1(1:200, Invitrogen) or anti-Occludin (1:200, Invitrogen) or anti-ZO1 (1:200,Thermo Fisher Scientific) primary antibodies for 16h. After washing with PBS, the liver sections were stained with secondary AlexaFluor 647-conjugated goat anti-mouse or anti-rabbit antibodies (1:500, Thermo Fisher Scientific) for 2h. Nuclei were stained with Hoechst dye. Liver sections were then washed three times, 5min each, with PBS. Slides were mounted by mounting solution and images were acquired by Nikon A1 Spectral Confocal Microscope.

Bioluminescence Imaging

EF transgenic mice Rosa26-Fluc, mCD81/hEL2[h/h] mOCLN/hEL2[h/h] Rosa26-Fluc were injected intravenously with the indicated doses of HCV-CRE**.** Rosa26-

Fluc mice were injected with 10^{11} adenovirus PFU 24 hours prior to intravenous injection with with 2 x 10^7 $TCID_{50}$ HCV-CRE**.** At 72 hours post infection, mice were anesthetized using ketamine/xylazine and injected intraperitoneally with 1.5 mg luciferin (Caliper Lifesciences). For the ex vivo measurements of luciferase activity across different tissues, the indicated organs were extracted from mCD81/hEL2[h/h] mOCLN/hEL2[h/h] Rosa26-Fluc and Rosa26-Fluc mice 72 hours post infection and placed in PBS containing luciferin (0.15 mg/ml) and luminescent activity measured. Bioluminescence was measured using an IVIS Lumina II platform (Caliper Lifesciences).

Results:

Physiologic expression of humanized CD81 and OCLN transcripts across multiple tissues

HCV entry factors are expressed at finely controlled levels in the liver and other tissues. In order to achieve more physiological expression, we undertook a knock-in approach. The low efficiency of entry mediated by murine CD81 and OCLN has been mapped to divergence in the respective second extracellular loops (18, 19). Thus, we reasoned that minimal replacements might be sufficient to permit HCV infection while preserving murine-specific intracellular domains. The large extracellular loop (amino acids 115-202) of murine CD81 was replaced by knocking in human exons 6 and 7 (**Figure 1A, 1C**). Similarly, exon 3 of OCLN, which encodes the second extracellular loop, was replaced with the human sequence (**Figure 1B, 1D**). Chimeric founder mice, termed mCD81/hEL2[h/m] and mOCLN/hEL2[h/m] respectively, were identified and backcrossed to the C57BL/6 background. Offspring did not show any gross phenotype and was born in the expected Mendelian ratios. CD81 is expressed in all nucleated cells and OCLN is an integral molecule of all tight junction complexes. To ascertain a similarly broad tissue expression of the humanized allele we subjected brain, skin, intestine, stomach, heart, lung, spleen, kidney and liver tissue of wild-type, mCD81/hEL2[h/h] and mOCLN/hEL2[h/h] to quantitative RT-PCR analysis using allele specific-primers. Both mutant mouse strains showed largely similar CD81

or OCLN tissue expression as to wild-type mice (**Figure 2A, B**) with slightly lower transcript levels in liver, spleen and lung tissue. We did not observe any difference in the level of expression in mice homozygous or heterozygous (data not shown) for the respective chimeric alleles.

mCD81/hEL2[h/h] and mOCLN/hEL2[h/h] mice do not show any overt pathophysiological phenotype

Besides its role as entry factor for human hepatotropic pathogens such as HCV and *Plasmodium falciparum* (29), CD81 is a cell surface molecule expressed on many cell types and associated with the CD19/CD21/Leu13 signal-transducing complex on B cells. Conceivably, humanizing the second extracellular loop of mouse CD81 may interfere with its endogenous functions and possibly could resemble phenotypically CD81 deficient (CD81-/-) mice. CD81-/- are reported to have decreased expression of CD19 and reduced numbers of peritoneal B-1 cells (30-32). Thus, we compared lymphocyte frequencies in wild-type and mCD81/hEL2[h/h] mice. CD8 and CD4 T cells frequencies were unaltered in the thymus (**Figure 3A**, top panels) and the spleen (**Figure 3A**, top panels) both mutant and wild-type animals. mCD81/hEL2[h/h] mice had normal frequencies of $IgM^{-}B220^{lo}$ cells (pro-B cells), $IgM^{-}B220^{int}$ cells (pre-B cells), $IgM^{+}B220^{int}$ (immature B cells), and $IgM^{+}B220^{hi}$ cells (mature B cells) and CD19 expression was normal (**Figure 3B**) . Thus, all stages of B cell development in the bone marrow appear to be normal. Furthermore, besides a slight (two fold) increase in the frequency of B1a cells in the peritoneum, overall numbers of B1 and B2 cells were similar wild-type and mCD81/hEL2[h/h] mice (**Figure 3C**).

OCLN is an integral membrane protein with four transmembrane domains that is exclusively localized at TJ strands. The two extracellular loops form homotypic interactions to stabilize TJs (33). To ensure that humanization of the second extracellular loop does not affect OCLN physiological functions we subjected tissue from mOCLN/hEL2[h/h] and wild-type mice to histological analysis. It was previously shown that OCLN deficient (OCLN-/-) mice exhibit histological

abnormalities in several tissues, i.e., chronic inflammation and hyperplasia of the gastric epithelium, calcification in the brain, testicular atrophy, loss of cytoplasmic granules in striated duct cells of the salivary gland, and thinning of the compact bone (34). In contrast mOCLN/hEL2[h/h] mice developed normally, nursed their offspring and did not show any of the histopathological features of OCLN deficient mice. Staining of OCLN, claudin-1 (CLDN1) and ZO-1 in liver sections, all of which are TJ components, was indistinguishable between mOCLN/hEL2[m/m] and mOCLN/hEL2[h/h] mice (**Figure 3D**). Overall, these data demonstrate that humanization of the second extracellular loop of both CD81 and OCLN does not seem to impair the endogenous functions.

Dose dependent uptake of HCV into mCD81/hEL2[h/h] mOCLN/hEL2[h/h] mice

Next we aimed to test whether the minimal humanization of the murine CD81 and OCLN alleles would be sufficient to facilitate viral uptake into murine hepatocytes *in vivo*. We have previously shown that adenoviral delivery or transgenic expression of full length human CD81 and OCLN is sufficient to enable HCV glycoprotein mediated uptake (21, 22, 35). To assess the ability to mCD81/hEL2[h/h] mOCLN/hEL2[h/h] double knock-in mice to support HCV uptake *in vivo* we employed a cellularly encoded reporter which can be activated by co-expression of Cre recombinase (21, 35, 36). mCD81/hEL2[h/h] mOCLN/hEL2[h/h] were intercrossed with the Gt(ROSA)26Sor$^{tm1(Luc)Kaelin}$ (Rosa26-Fluc) mouse strain (26) harboring a loxP-flanked luciferase reporter. Resultant offspring was infected with increasing doses tissue culture infectious doses (TCID) of a bicistronic HCV genome expressing Cre recombinase (BiCre-Jc1, abbreviated HCV-Cre), which is designed to activate a luminescent reporter. *In vivo* luminescence imaging demonstrated a significant increase in relative photon flux in the entry factor double knockin (EFKI) mice 72 hours post infection (**Figure 4A, B**). The signal increased roughly 3 fold over background following infection with the highest dose tested (3x10E7 TCID) (**Figure 4B**), demonstrating that uptake efficiency is dose dependent. This dose dependency is consistent with what has been previously reported in HCV entry factor transgenic mice (22)

or animals expressing CD81 and OCLN (21) in their livers after adenoviral delivery. Of note, reporter activity was largely limited to the liver and we only observed a slight activation of the reporter in the spleen and kidney of the reporter in but not in other, non-hepatic tissues, were the humanized alleles may also be expressed (**Figure. 4C**).

mCD81/hEL2[h/h] mOCLN/hEL2[h/h] double knock-in mice support HCV entry at similar levels as mice expressing adenovirally-delivered or transgenically CD81 and OCLN

Lastly, we aimed to compare whether the efficiency of HCV into murine hepatocytes would differ across animals in which human(ized) CD81 and OCLN is (over-)expressed by different means. mCD81/hEL2[h/h] mOCLN/hEL2[h/h] mice and animals expressing full length human CD81 and OCLN adenovirally off a cytomegalovirus (CMV) promoter or transgenically off a mouse albumin promoter (all on the Rosa26-Fluc background) were injected with 2x10E7 TCID of BiCre-Jc1 and the bioluminescence signal quantified after 72 hours (**Figure 5**). The bioluminescence signal increased 2-3 fold over background and was largely equivalent across all three entry models. Collectively, these data demonstrate that minimal humanization of the second extracellular loops is sufficient to facilitate entry of HCV harboring diverse envelope proteins into hepatocytes but presumably not in extrahepatic tissues.

Discussion:

Use of great apes in biomedical research is heavily scrutinized and either banned or federal funding has ceased. In search for alternative models a variety of approaches have been taken (reviewed in (4)). Some studies suggested that tree shrews (*Tupaia belangeri*) can become chronically infected with HCV (37) (38, 39) and even develop fibrosis (39) but this model has not found wide spread use yet. HCV-like viruses have been more recently identified in a variety of species including horses, dogs, rat and mice but it is unclear whether such related hepaciviruses cause clinical symptoms similar to hepatitis C and thus could be

used as surrogate models (40). A variety of other approaches have been pursued focusing on modifying the (murine) host environment in a way that it comes more conducive to HCV infection. Mice engrafted with human hepatocytes have been shown to be susceptible HCV (25, 41-43). Despite their utility for studying a variety of human hepatotropic pathogens, such human liver chimeric mice have not found wide-spread use as they can only be produced at low throughput, and their generation is expensive and requires considerable technical skills. Alternatively, systematic analysis and identification of some of the barriers on interspecies transmission of HCV to classically non-permissive species, in particular mice, has spurned genetic humanization efforts. After the discovery that human CD81 and OCLN comprise the minimal set of human specific factors requires for viral entry into mouse cell lines (12) it was demonstrated that adenovirally-mediated (21) or transgenic overexpression (22) of these factors enabled HCV entry *in vivo*. Caveats of these two systems are the non-physiologically high and the exclusive expression in hepatocytes. Adenovirally mediated expression of human CD81 and OCLN can exceed endogenous expression levels of mouse 100-1000 fold (21) and transgenic expression under the control of a mouse albumin promoter still results in 10-fold overexpression (10). Furthermore, the intracellular domains of the full-length human orthologues may interact less efficiently with the murine proteins that usually bind to their respective adaptor proteins. To address the shortcomings mice whose second extracellular loops of CD81 and OCLN were humanized. mCD81/hEL2 mOCLN/hEL2 double knock-in mice develop normally and the minimal loop humanization appears to be sufficient to facilitate HCV uptake into murine hepatocytes. Humanization of the second extracellular loops does not impair the respective endogenous functions of CD81 and OCLN in vivo. Conceivably, the phenotype of these mutant mice would have resembled animals with targeted disruptions of the CD81 (30-32) and OCLN (34), which were previously reported. However, our analysis demonstrates that the loop replacements do not alter noticeably B lymphocyte or tight junction biology.

Based on several clinical conditions it has previously been speculated that extrahepatic sites of HCV infection may exist. For example a potential involvement of the central nervous system (CNS) was based on observations that chronic HCV carriers frequently become encephalopathic and develop neuropsychiatric disorders (44). HCV RNA has been detected brain tissue from HCV infected individuals (45), but contamination of samples collected post mortem after the blood-brain-barrier has broken down is a confounding problem. Additional, evidence for the CNS as a putative HCV reservoir stemmed from *in vitro* studies showing that HCV can enter human peripheral neuro-blastoma and -epithelioma cells *in vitro* (46, 47). However, currently there is no direct evidence of active HCV RNA replication patient-derived cells of the CNS. HCV RNA has also been shown to be associated with various hematopoietically derived cells, such as B and T lymphocytes, monocytes, and dendritic cells. This led to the hypothesis that HCV may infect these populations, triggering lymphoproliferative disorders which are frequently observed in chronic HCV carriers. However, attempts to infect human peripheral blood mononuclear cells (PBMCs) largely with cell-culture derived HCV failed (48), suggesting that HCV particles and/or RNA may adhere to these cells but not efficiently enter. HCV proteins have also been detected in epithelial cells of intestinal specimens collected from HCV infected patients (49) and *in vitro* experiments provided evidence that can enter the epithelial-derived colorectal adenocarcinoma Caco-2 cell line (50).

It remains controversial whether HCV infect non-parenchymal cells in vivo such putative extrahepatic sites have any clinical relevance. CD81 is ubiquitously expressed in almost all nucleated cells and OCLN is part of all tight junction complexes present in polarized cell layers. Interestingly, alternative splice forms of OCLN have been described which are differentially expressed across tissues and thus might contribute to HCV tissue tropism (51). However, while CLDN1 and SCARBI are expressed in a variety of non-hepatic tissues the combination of both at high levels is only present in the liver, which may contribute largely to HCV's tissue specificity at the entry level. Consistently, we observed HCV uptake primary in the liver and to a much lesser extend in the spleen and kidneys of

HCV infection double knock-in mice. The limited evidence for HCV uptake in non-hepatic tissues may, however, be owed to the limits of detection of the assays employed here. In future studies, our model may lend itself further explore HCV tissue tropism further.

Acknowledgements:

The authors thank Jenna Gaska for edits and critical discussion of the manuscript.

Funding information:

This study is supported by grants from the National Institutes of Health (R01 AI079031, R01 AI107301, R21AI117213 to AP), a Research Scholar Award from the American Cancer Society (RSG-15-048-01-MPC to AP), a Burroughs Wellcome Fund Award for Investigators in Pathogenesis (to AP). Q.D. is a recipient of a postdoctoral fellowship from the New Jersey Commission on Cancer Research and M.v.S. from the German Research Foundation (Deutsche Forschungsgemeinschaft). L.S. is a fellow of the German National Merit Foundation and was supported by a stipend from the Organization of Supporters of the Hannover Medical School ("Gesellschaft der Freunde der Medizinischen Hochschule Hannover e.V.").

References:

1. **Lindenbach BD, Rice CM.** 2001. *Flaviviridae*: The viruses and their replication, p 991-1041. *In* Knipe DM, Howley PM (ed), Fields Virology, Fourth ed, vol 1. Lippincott-Raven Publishers, Philadelphia.
2. **Westbrook RH, Dusheiko G.** 2014. Natural history of hepatitis C. J Hepatol **61:**S58-68.
3. **Wang LS, D'Souza LS, Jacobson IM.** 2016. Hepatitis C-A clinical review. J Med Virol **88:**1844-1855.
4. **von Schaewen M, Ploss A.** 2014. Murine models of hepatitis C: what can we look forward to? Antiviral Res **104:**15-22.
5. **Ding Q, von Schaewen M, Ploss A.** 2014. The Impact of Hepatitis C Virus Entry on Viral Tropism. Cell Host Microbe **16:**562-568.
6. **Barth H, Schafer C, Adah MI, Zhang F, Linhardt RJ, Toyoda H, Kinoshita-Toyoda A, Toida T, Van Kuppevelt TH, Depla E, Von Weizsacker F, Blum HE, Baumert TF.** 2003. Cellular binding of hepatitis C virus envelope glycoprotein E2 requires cell surface heparan sulfate. J Biol Chem **278:**41003-41012.
7. **Agnello V, Abel G, Elfahal M, Knight GB, Zhang QX.** 1999. Hepatitis C virus and other flaviviridae viruses enter cells via low density lipoprotein receptor. Proc Natl Acad Sci U S A **96:**12766-12771.
8. **Pileri P, Uematsu Y, Campagnoli S, Galli G, Falugi F, Petracca R, Weiner AJ, Houghton M, Rosa D, Grandi G, Abrignani S.** 1998. Binding of hepatitis C virus to CD81. Science **282:**938-941.
9. **Scarselli E, Ansuini H, Cerino R, Roccasecca RM, Acali S, Filocamo G, Traboni C, Nicosia A, Cortese R, Vitelli A.** 2002. The human scavenger receptor class B type I is a novel candidate receptor for the hepatitis C virus. EMBO Journal **21:**5017-5025.
10. **Evans MJ, von Hahn T, Tscherne DM, Syder AJ, Panis M, Wolk B, Hatziioannou T, McKeating JA, Bieniasz PD, Rice CM.** 2007. Claudin-1 is a hepatitis C virus co-receptor required for a late step in entry. Nature **446:**801-805.
11. **Liu S, Yang W, Shen L, Turner JR, Coyne CB, Wang T.** 2009. Tight junction proteins claudin-1 and occludin control hepatitis C virus entry and are downregulated during infection to prevent superinfection. J Virol **83:**2011-2014.
12. **Ploss A, Evans MJ, Gaysinskaya VA, Panis M, You H, de Jong YP, Rice CM.** 2009. Human occludin is a hepatitis C virus entry factor required for infection of mouse cells. Nature **457:**882-886.
13. **Lupberger J, Zeisel MB, Xiao F, Thumann C, Fofana I, Zona L, Davis C, Mee CJ, Turek M, Gorke S, Royer C, Fischer B, Zahid MN, Lavillette D, Fresquet J, Cosset FL, Rothenberg SM, Pietschmann T, Patel AH, Pessaux P, Doffoel M, Raffelsberger W, Poch O, McKeating JA, Brino L, Baumert TF.** 2011. EGFR and EphA2 are host factors for hepatitis C virus entry and possible targets for antiviral therapy. Nat Med **17:**589-595.

14. **Sainz B, Jr., Barretto N, Martin DN, Hiraga N, Imamura M, Hussain S, Marsh KA, Yu X, Chayama K, Alrefai WA, Uprichard SL.** 2012. Identification of the Niemann-Pick C1-like 1 cholesterol absorption receptor as a new hepatitis C virus entry factor. Nat Med **18:**281-285.
15. **Martin DN, Uprichard SL.** 2013. Identification of transferrin receptor 1 as a hepatitis C virus entry factor. Proc Natl Acad Sci U S A **110:**10777-10782.
16. **Wu X, Lee EM, Hammack C, Robotham JM, Basu M, Lang J, Brinton MA, Tang H.** 2014. Cell death-inducing DFFA-like effector b is required for hepatitis C virus entry into hepatocytes. J Virol **88:**8433-8444.
17. **Li Q, Sodroski C, Lowey B, Schweitzer CJ, Cha H, Zhang F, Liang TJ.** 2016. Hepatitis C virus depends on E-cadherin as an entry factor and regulates its expression in epithelial-to-mesenchymal transition. Proc Natl Acad Sci U S A **113:**7620-7625.
18. **Higginbottom A, Quinn ER, Kuo CC, Flint M, Wilson LH, Bianchi E, Nicosia A, Monk PN, McKeating JA, Levy S.** 2000. Identification of amino acid residues in CD81 critical for interaction with hepatitis C virus envelope glycoprotein E2. J Virol **74:**3642-3649.
19. **Michta ML, Hopcraft SE, Narbus CM, Kratovac Z, Israelow B, Sourisseau M, Evans MJ.** 2010. Species-specific regions of occludin required by hepatitis C virus for cell entry. J Virol **84:**11696-11708.
20. **Vogt A, Scull MA, Friling T, Horwitz JA, Donovan BM, Dorner M, Gerold G, Labitt RN, Rice CM, Ploss A.** 2013. Recapitulation of the hepatitis C virus life-cycle in engineered murine cell lines. Virology **444:**1-11.
21. **Dorner M, Horwitz JA, Robbins JB, Barry WT, Feng Q, Mu K, Jones CT, Schoggins JW, Catanese MT, Burton DR, Law M, Rice CM, Ploss A.** 2011. A genetically humanized mouse model for hepatitis C virus infection. Nature **474:**208-211.
22. **Dorner M, Horwitz JA, Donovan BM, Labitt RN, Budell WC, Friling T, Vogt A, Catanese MT, Satoh T, Kawai T, Akira S, Law M, Rice CM, Ploss A.** 2013. Completion of the entire hepatitis C virus life cycle in genetically humanized mice. Nature **501:**237-241.
23. **Giang E, Dorner M, Prentoe JC, Dreux M, Evans MJ, Bukh J, Rice CM, Ploss A, Burton DR, Law M.** 2012. Human broadly neutralizing antibodies to the envelope glycoprotein complex of hepatitis C virus. Proceedings of the National Academy of Sciences of the United States of America **109:**6205-6210.
24. **Anggakusuma, Colpitts CC, Schang LM, Rachmawati H, Frentzen A, Pfaender S, Behrendt P, Brown RJ, Bankwitz D, Steinmann J, Ott M, Meuleman P, Rice CM, Ploss A, Pietschmann T, Steinmann E.** 2014. Turmeric curcumin inhibits entry of all hepatitis C virus genotypes into human liver cells. Gut **63:**1137-1149.
25. **de Jong YP, Dorner M, Mommersteeg MC, Xiao JW, Balazs AB, Robbins JB, Winer BY, Gerges S, Vega K, Labitt RN, Donovan BM, Giang E, Krishnan A, Chiriboga L, Charlton MR, Burton DR,**

Baltimore D, Law M, Rice CM, Ploss A. 2014. Broadly neutralizing antibodies abrogate established hepatitis C virus infection. Sci Transl Med **6:**254ra129.

26. **Safran M, Kim WY, Kung AL, Horner JW, DePinho RA, Kaelin WG, Jr.** 2003. Mouse reporter strain for noninvasive bioluminescent imaging of cells that have undergone Cre-mediated recombination. Mol Imaging **2:**297-302.
27. **Lindenbach BD, Evans MJ, Syder AJ, Wolk B, Tellinghuisen TL, Liu CC, Maruyama T, Hynes RO, Burton DR, McKeating JA, Rice CM.** 2005. Complete Replication of Hepatitis C Virus in Cell Culture. Science **309:**623-626.
28. **Schoggins JW, Gall JG, Falck-Pedersen E.** 2003. Subgroup B and F fiber chimeras eliminate normal adenovirus type 5 vector transduction in vitro and in vivo. J Virol **77:**1039-1048.
29. **Silvie O, Rubinstein E, Franetich JF, Prenant M, Belnoue E, Renia L, Hannoun L, Eling W, Levy S, Boucheix C, Mazier D.** 2003. Hepatocyte CD81 is required for Plasmodium falciparum and Plasmodium yoelii sporozoite infectivity. Nat Med **9:**93-96.
30. **Maecker HT, Levy S.** 1997. Normal lymphocyte development but delayed humoral immune response in CD81-null mice. J Exp Med **185:**1505-1510.
31. **Tsitsikov EN, Gutierrez-Ramos JC, Geha RS.** 1997. Impaired CD19 expression and signaling, enhanced antibody response to type II T independent antigen and reduction of B-1 cells in CD81-deficient mice. Proc Natl Acad Sci U S A **94:**10844-10849.
32. **Miyazaki T, Muller U, Campbell KS.** 1997. Normal development but differentially altered proliferative responses of lymphocytes in mice lacking CD81. EMBO J **16:**4217-4225.
33. **Van Itallie CM, Anderson JM.** 2014. Architecture of tight junctions and principles of molecular composition. Semin Cell Dev Biol **36:**157-165.
34. **Saitou M, Furuse M, Sasaki H, Schulzke JD, Fromm M, Takano H, Noda T, Tsukita S.** 2000. Complex phenotype of mice lacking occludin, a component of tight junction strands. Mol Biol Cell **11:**4131-4142.
35. **Dorner M, Rice CM, Ploss A.** 2012. Study of hepatitis C virus entry in genetically humanized mice. Methods doi:10.1016/j.ymeth.2012.05.010.
36. **von Schaewen M, Ding Q, Ploss A.** 2014. Visualizing hepatitis C virus infection in humanized mice. J Immunol Methods **410:**50-59.
37. **Xie ZC, Riezu-Boj JI, Lasarte JJ, Guillen J, Su JH, Civeira MP, Prieto J.** 1998. Transmission of hepatitis C virus infection to tree shrews. Virology **244:**513-520.
38. **Xu X, Chen H, Cao X, Ben K.** 2007. Efficient infection of tree shrew (Tupaia belangeri) with hepatitis C virus grown in cell culture or from patient plasma. J Gen Virol **88:**2504-2512.
39. **Amako Y, Tsukiyama-Kohara K, Katsume A, Hirata Y, Sekiguchi S, Tobita Y, Hayashi Y, Hishima T, Funata N, Yonekawa H, Kohara M.** 2010. Pathogenesis of hepatitis C virus infection in Tupaia belangeri. J Virol **84:**303-311.

40. **Pfaender S, Brown RJ, Pietschmann T, Steinmann E.** 2014. Natural reservoirs for homologs of hepatitis C virus. Emerg Microbes Infect **3:**e21.
41. **Mercer DF, Schiller DE, Elliott JF, Douglas DN, Hao C, Rinfret A, Addison WR, Fischer KP, Churchill TA, Lakey JR, Tyrrell DL, Kneteman NM.** 2001. Hepatitis C virus replication in mice with chimeric human livers. Nat Med **7:**927-933.
42. **Meuleman P, Libbrecht L, De Vos R, de Hemptinne B, Gevaert K, Vandekerckhove J, Roskams T, Leroux-Roels G.** 2005. Morphological and biochemical characterization of a human liver in a uPA-SCID mouse chimera. Hepatology **41:**847-856.
43. **Bissig KD, Wieland SF, Tran P, Isogawa M, Le TT, Chisari FV, Verma IM.** 2010. Human liver chimeric mice provide a model for hepatitis B and C virus infection and treatment. J Clin Invest **120:**924-930.
44. **Forton DM, Taylor-Robinson SD, Thomas HC.** 2003. Cerebral dysfunction in chronic hepatitis C infection. J Viral Hepat **10:**81-86.
45. **Fishman SL, Murray JM, Eng FJ, Walewski JL, Morgello S, Branch AD.** 2008. Molecular and bioinformatic evidence of hepatitis C virus evolution in brain. J Infect Dis **197:**597-607.
46. **Burgel B, Friesland M, Koch A, Manns MP, Wedemeyer H, Weissenborn K, Schulz-Schaeffer WJ, Pietschmann T, Steinmann E, Ciesek S.** 2010. Hepatitis C virus enters human peripheral neuroblastoma cells - evidence for extra-hepatic cells sustaining hepatitis C virus penetration. J Viral Hepat doi:JVH1339 [pii]
47. **Fletcher NF, Yang JP, Farquhar MJ, Hu K, Davis C, He Q, Dowd K, Ray SC, Krieger SE, Neyts J, Baumert TF, Balfe P, McKeating JA, Wong-Staal F.** 2010. Hepatitis C virus infection of neuroepithelioma cell lines. Gastroenterology **139:**1365-1374.
48. **Marukian S, Jones CT, Andrus L, Evans MJ, Ritola KD, Charles ED, Rice CM, Dustin LB.** 2008. Cell culture-produced hepatitis C virus does not infect peripheral blood mononuclear cells. Hepatology **48:**1843-1850.
49. **Deforges S, Evlashev A, Perret M, Sodoyer M, Pouzol S, Scoazec JY, Bonnaud B, Diaz O, Paranhos-Baccala G, Lotteau V, Andre P.** 2004. Expression of hepatitis C virus proteins in epithelial intestinal cells in vivo. J Gen Virol **85:**2515-2523.
50. **Mee CJ, Grove J, Harris HJ, Hu K, Balfe P, McKeating JA.** 2008. Effect of cell polarization on hepatitis C virus entry. J Virol **82:**461-470.
51. **Kohaar I, Ploss A, Korol E, Mu K, Schoggins JW, O'Brien TR, Rice CM, Prokunina-Olsson L.** 2010. Splicing diversity of the human OCLN gene and its biological significance for hepatitis C virus entry. J Virol **84:**6987-6994.

630 **Figure legends:**

631 **Figure 1: Schematic representation of humanized CD81 and OCLN alleles**
632 **and native tissue expression profiles of humanized CD81 and OCLN alleles**
633 Schematic representation of the mCD81/hEL2 (**A.**) and mOCLN/hEL2 (**B.**)
634 proteins and alignments of sequences of the second extracellular loops of
635 mouse, human and humanized proteins. Differences between the human and
636 mouse sequences are bolded, the residues that were shown to be critical for
637 HCV uptake are underlined. Schematics detailing the targeting strategy to
638 generate the mCD81/hEL2[h/h] (**C.**) or mOCLN/hEL2[h/h] knock-in mice(**D.**).
639
640 **Figure 2: Expression humanized CD81 and OCLN alleles in entry factor**
641 **knock-in mice.** Quantification of the wild-type and humanized transcripts (**A.**
642 mCD81/hEL2[h/h], **B.** mOCLN/hEL2[h/h]) in different tissues. Shown as mean ±
643 SD of at least 3 experiments. Statistical analysis was performed using a one-
644 tailed Student t test.(* $p<0.05$, ** $p<0.01$ and *** $p<0.001$), n.s. = not statistically
645 significant.
646
647 **Figure 3: Humanization of the second extracellular loops of CD81 and**
648 **OCLN does not interfere with the endogenous functions of these molecules**
649 **A.** Flow cytometry analysis of thymocytes (*top panels*) and splenocytes (*bottom*
650 *panels*) from wild-type (WT) and mCD81/hEL2[h/h]. **B.** Flow cytometry analysis
651 of bone-marrow cells (**B.**) and peritoneal lavage cells (**C.**) from wild-type (WT)
652 and mCD81/hEL2[h/h]. Shown are representative flowcytometric plots and
653 frequencies (mean ± SD). **D.** Confocal microscopy images of thin sections (6 µm)
654 of livers from mOCLN/hEL2[m/m] (wild-type) or mOCLN/hEL2[h/h] stained with
655 antibodies against mouse OCLN (top), CLDN1 (middle) or ZO1 (bottom). To
656 visualize nuclei (blue) sections were stained with Hoechst dye.
657
658 **Figure 4: Activation of the bioluminescent reporter in HCV entry factor**
659 **knock-in mice is dependent on HCV dose. A.** Representative images of mock
660 (left) or HCV-Cre injected mOCLN/hEL2[m/m] mOCLN/hEL2[h/h] Rosa26-Fluc

mice. **B.** mOCLN/hEL2[m/m] mOCLN/hEL2[h/h] Rosa26-Fluc mice (n=3)) were injected with the indicated various doses of HCV-Cre. Data represent mean ± SD. Statistical significance was calculated by One-way ANOVA with Bonferroni's multiple comparison test. **C.** Luminescent reporter activation across different tissues. The indicated tissues from Rosa26-Fluc or mOCLN/hEL2[m/m] mOCLN/hEL2[h/h] Rosa26-Fluc mice were extracted and luminescent activity measured *ex vivo*. All bioluminescent signals were quantified 72 hours following infection. Data represent mean ± SD. Statistical analysis was performed using a one-tailed Student t test. (* $p<0.05$, ** $p<0.01$ and *** $p<0.001$), n.s. = not statistically significant.

Figure 5: Similar uptake efficiency of HCV into different mouse models expressing HCV entry factors. Rosa26-Fluc mice were injected 1x10E11 adenovirus (AdV) particles CD81 and OCLN and 24 hours later these mice, Alb-hCD81/hOCLN entry factor transgenic (EFT) Rosa26-Fluc and mOCLN/hEL2[m/m] mOCLN/hEL2[h/h] entry factor knock-in (EFKI) Rosa26-Fluc mice were infected with 2x10E7 TCID of HCV **(**n=3). The bioluminescent signal quantified 72 hours following infection. Data represent mean ± SD. Statistical significance was calculated by One-way ANOVA with Bonferroni's multiple comparison test.(* $p<0.05$, ** $p<0.01$ and *** $p<0.001$), n.s. = not statistically significant.

Fig.1

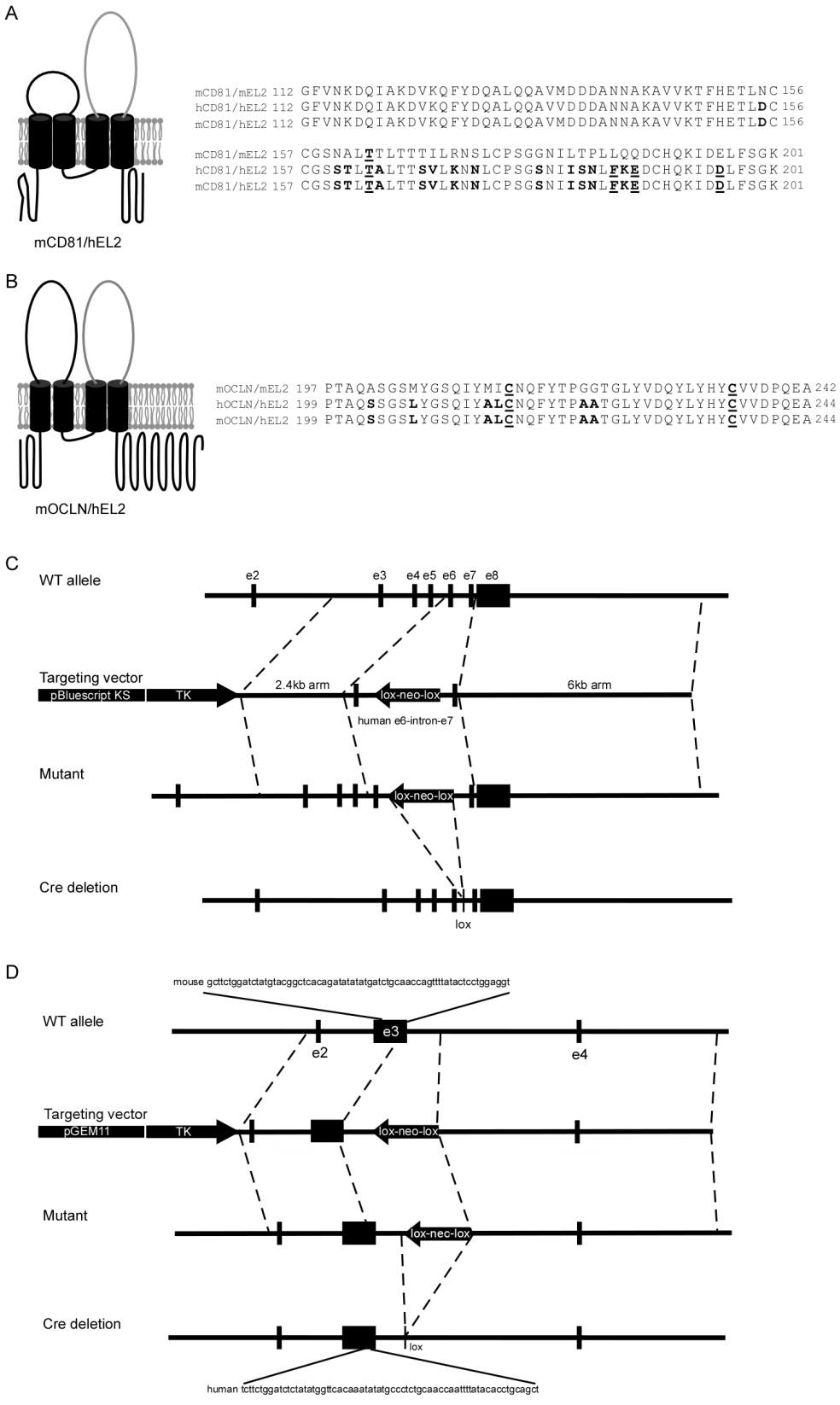

Fig.2

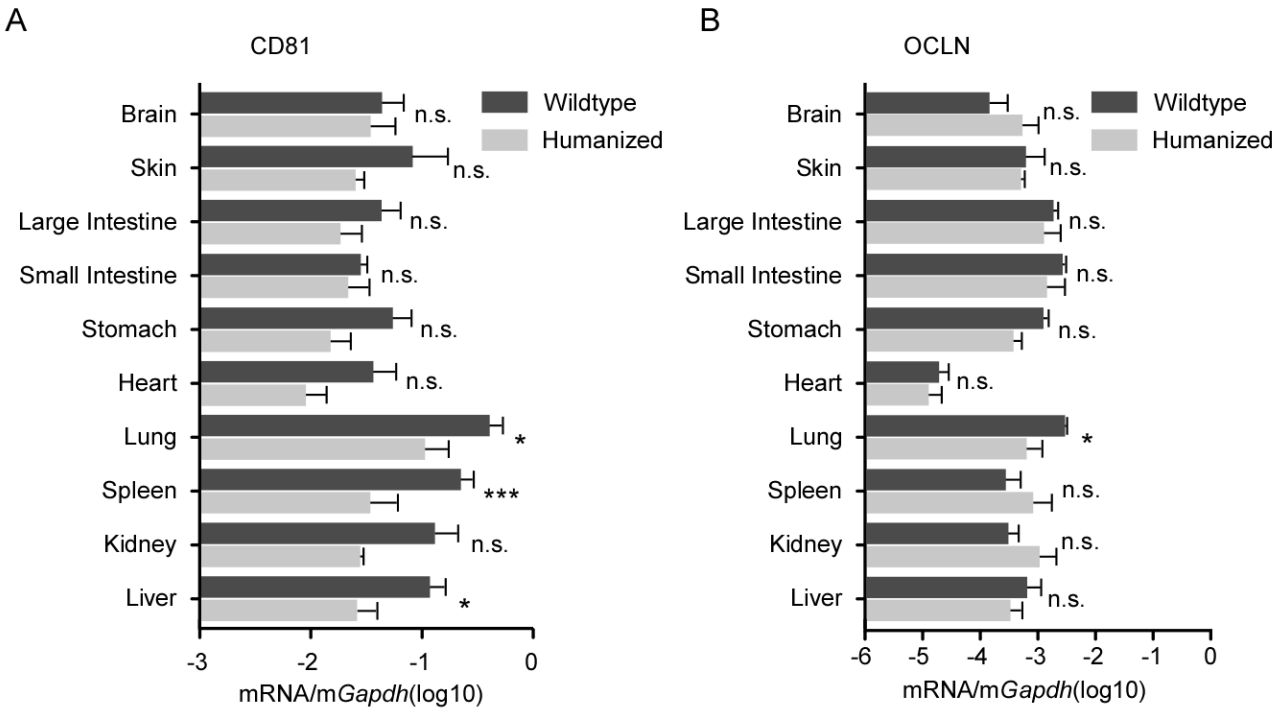

Fig.3

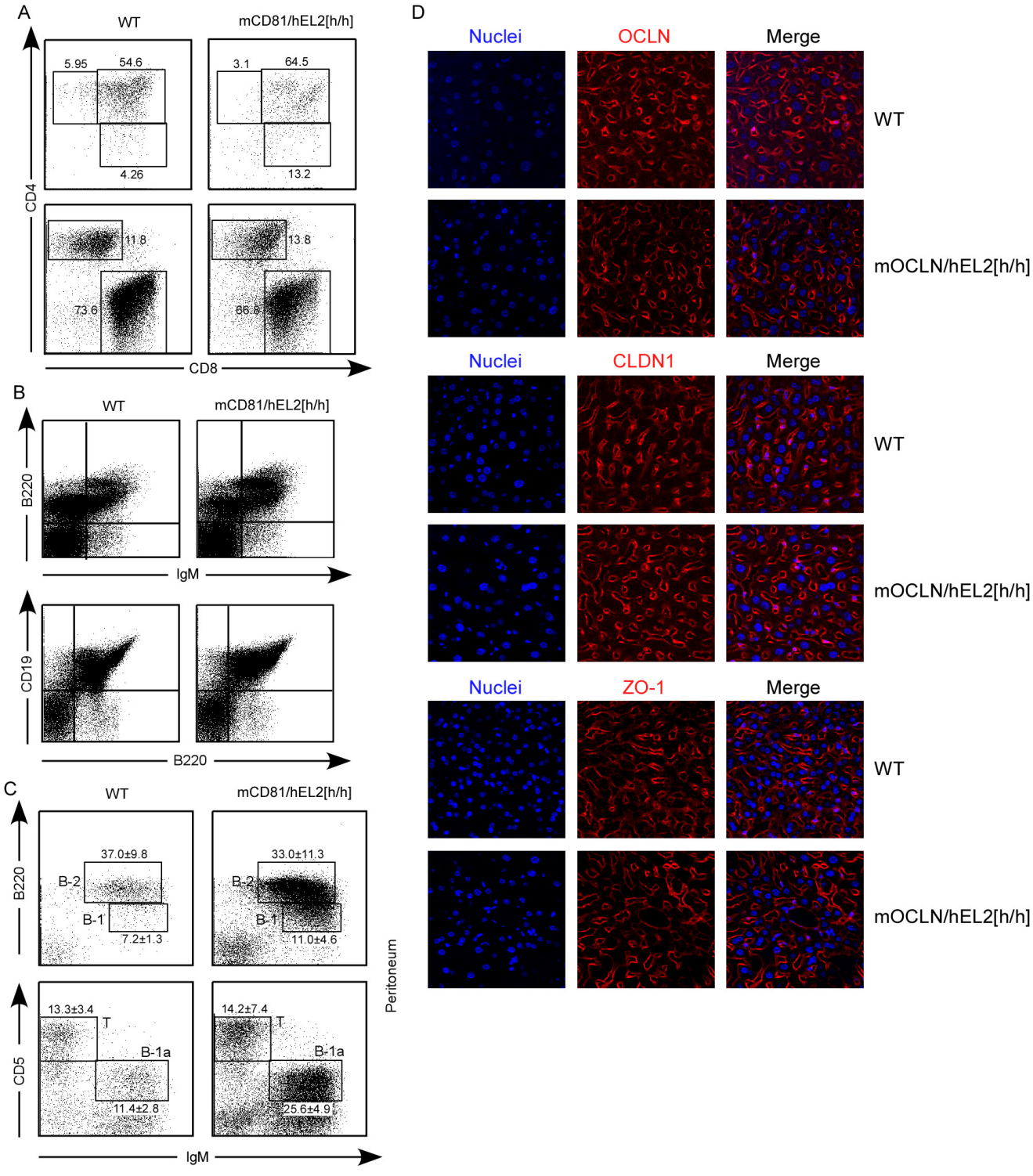

Fig.4

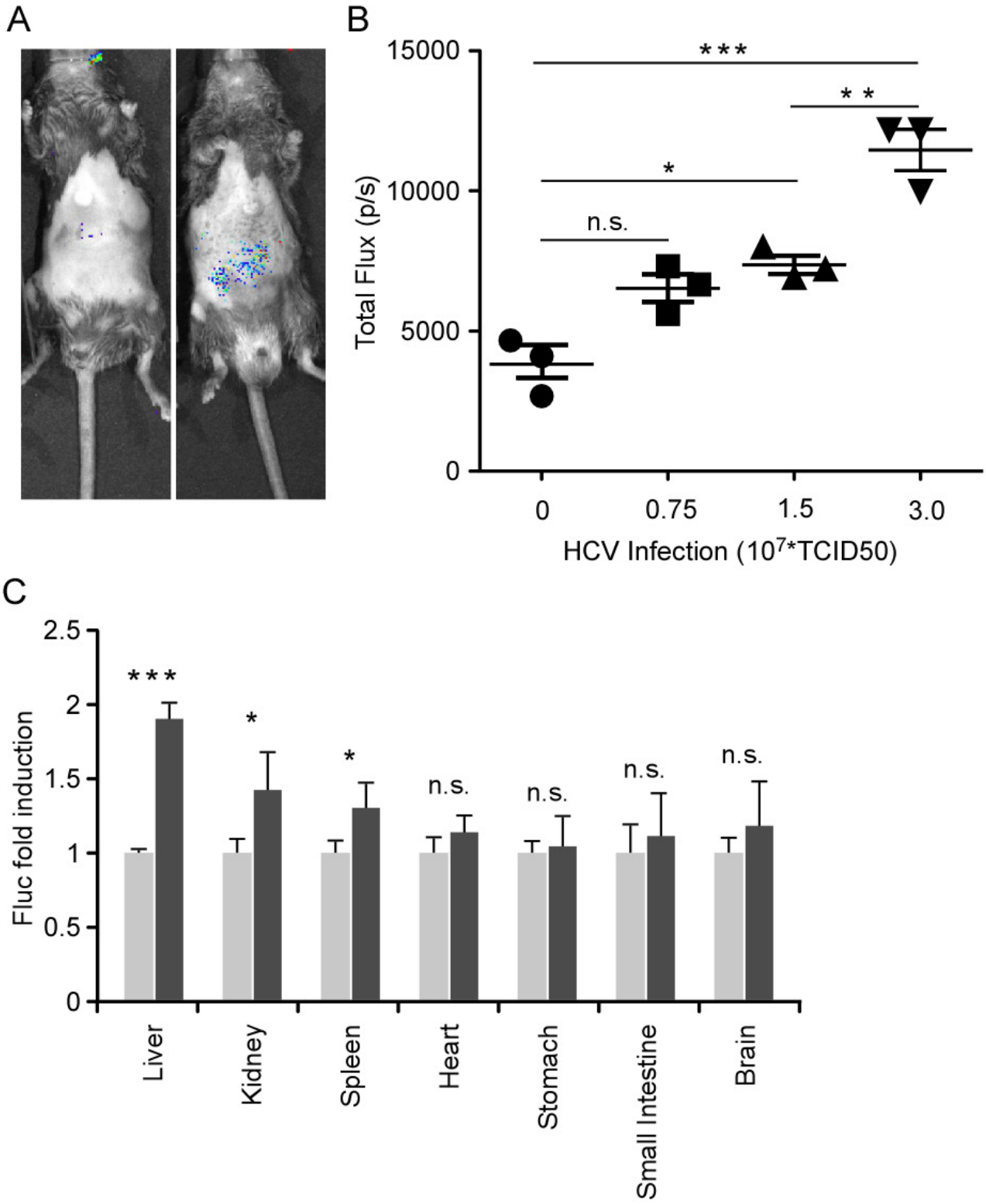

Fig.5

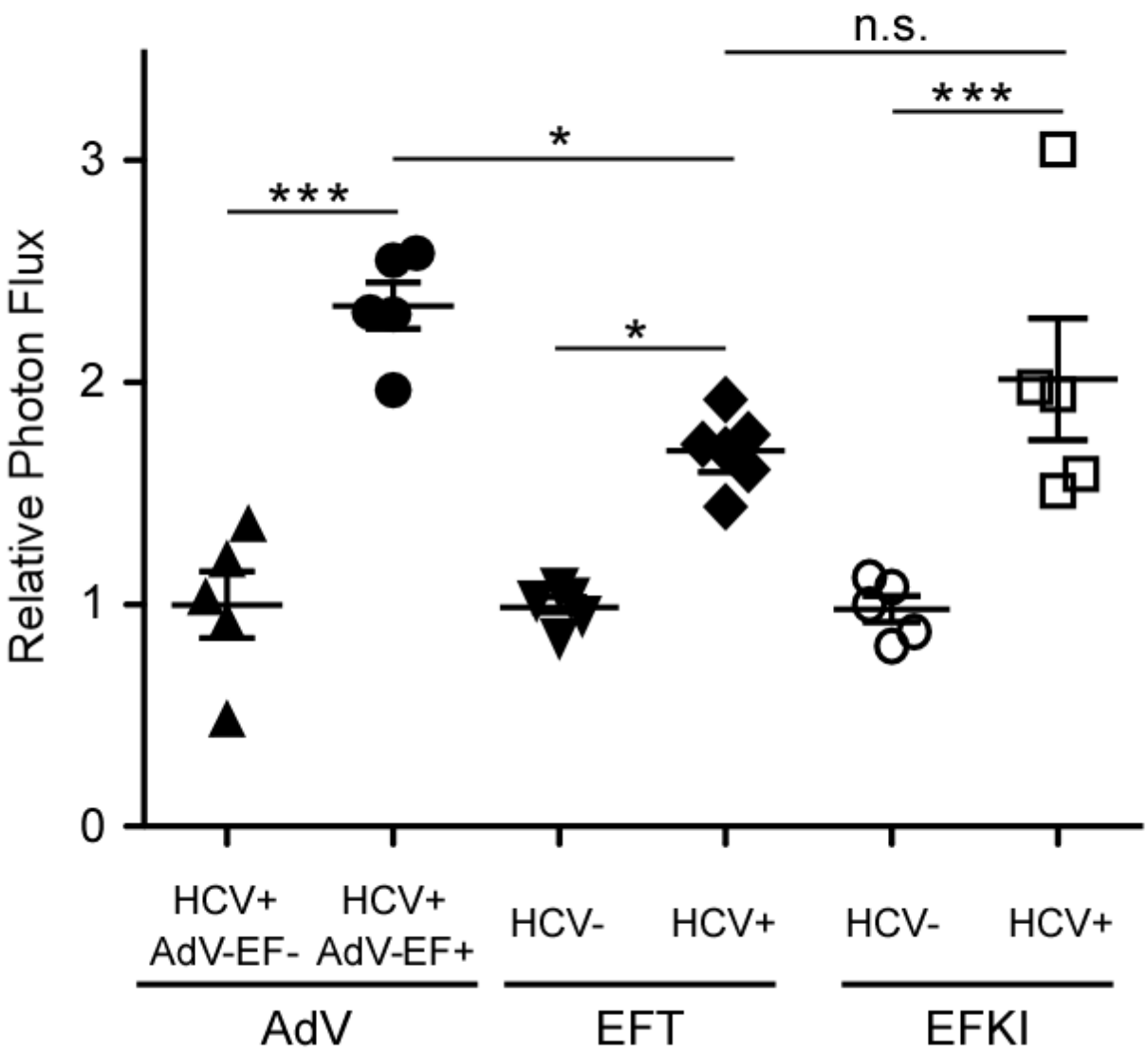

Gene	Forward Primer	Reverse Primer
mCD81/hEL2	CCAAGGCTGTGGTGAAGACTTTC	TGTTCTTGAGCACTGAGGTGGTC
mCD81/mEL2	CCAAGGCTGTGGTGAAGACTTTC	GGCTGTTCCTCAGTATGGTGGTAG
mOCLN/hEL2	AAATTGGTTGCAGAGGGCATAT	GTGTTTATTGCCACGATCGTGT
mOCLN/mEL2	AAACTGGTTGCAGATCATATAT	GTGTTTATTGCCACGATCGTGT
gapdh	ACGGCCAAATCCGTTCACACC	ACGGCCGCATCTTCTTGTGCA

Table 1: Primers used for the RT-qPCR analysis